

WAMS – based control of series FACTS devices installed in tie-lines of interconnected power system

ŁUKASZ NOGAL, JAN MACHOWSKI

*Institute of Electric Power Engineering, Warsaw University of Technology
00-662 Warszawa ul. Koszykowa 75*

e-mail: {lukas.nogal|jan.machowski}@ien.pw.edu.pl

(Received: 26.06.2010, revised: 01.10.2010)

Abstract: This paper addresses the state-variable stabilising control of the power system using such series FACTS devices as TCPAR installed in the tie-line connecting control areas in an interconnected power system. This stabilising control is activated in the transient state and is supplementary with respect to the main steady-state control designed for power flow regulation. Stabilising control laws, proposed in this paper, have been derived for a linear multi-machine system model using direct Lyapunov method with the aim to maximise the rate of energy dissipation during power swings and therefore maximise their damping. The proposed control strategy is executed by a multi-loop controller with frequency deviations in all control areas used as the input signals. Validity of the proposed state-variable control has been confirmed by modal analysis and by computer simulation for a multi-machine test system.

Key words: power system control, transient stability, FACTS, WAMS

1. Introduction

Traditionally the main control actions in a power system, such as transformer tap changes, have been achieved using mechanical devices and were therefore rather slow. However the continuing progress in the development of power electronics has enabled a number of devices to be developed, which provide the same functions but with much faster operation [1, 2]. Transmission networks equipped with such devices are referred to as FACTS (Flexible AC Transmission Systems).

Depending on the way FACTS devices are connected to a power system, they can be divided into shunt and series devices. Main shunt FACTS devices are reactive power compensators, energy storage (e.g. superconducting or battery based) and braking resistors. Among various series FACTS devices are series compensators, phase angle regulators TCPAR and power controllers UPFC. The most general FACTS device is the unified power flow controller (UPFC). UPFC is the most general FACTS device because it can execute the following control functions:

- (1) control of real power flows P by controlling the quadrature component $\text{Im}(\Delta \underline{V})$ of the booster voltage in the series part;

- (2) control of reactive power flows Q by controlling the direct component $\text{Re}(\Delta \underline{V})$ of the booster voltage in the series part,
- (3) control of the voltage V_i in the connection node by controlling the reactive current $\text{Im}(\underline{I}_{\text{shunt}})$ supplied by the network to the shunt part.

The first function (control of the quadrature component of the booster voltage) is equivalent to the function of another FACTS device TCPAR (Thyristor-Controlled Phase Angle Regulator). UPFC can also work similarly as the series compensator SSSC [2].

This paper deals with control of UPFC or TCPAR installed in tie-lines linking control areas in an interconnected power system.

The main aim of FACTS devices is normally steady-state control of a power system but, due to their fast response, FACTS devices can also be used for power system stability enhancement through improved damping of power swings. For this purpose the control circuits of FACTS devices are equipped with supplementary control loops [2, 3]. There are many publications describing various kinds of supplementary stabilising control. Usually they utilise as the input signals various locally measurable quantities like real and reactive power, voltage magnitude or current, local frequency etc. [4-7].

Simulation of the dynamic response of the power systems with UPFC or TCPAR in the tie-lines show that the use of the supplementary stabilising control based on locally measurable quantities is not satisfactory. It can force a parasitical interaction between load and frequency controllers (LFC) of individual control areas of the interconnected power system. This interaction deteriorates quality of the frequency regulation and disproves damping of the power swings. This results from the following fact that during the transient state (caused by a sudden disturbance in a power balance) the series FACTS devices installed in the tie-lines affect the values of tie-line power interchanges P_{tie} and therefore also the value of the area control error (ACE). This may affect the dynamics of secondary control executed by the central load and frequency controllers (LFC) [2].

To avoid the above mentioned problems a proper control algorithm has to be implemented at the regulator of the series FACTS devices installed in the tie-lines. This control should not deteriorate frequency and tie-line power interchange regulation process. Example of such control has been described in paper [19] where the authors proposed to solve the linear state-variable equations during the control process.

A different approach has been proposed in papers [8, 14] and book [2] written by one of the authors of this paper. In this book a new control structure, as illustrated in Fig. 1, has been proposed.

The main steady-state control loop (upper part of figure) is based on measuring a locally observable signal to be controlled by a FACTS device. For the thyristor-controlled phase angle regulator (TCPAR), it is real power in given transmission line. For UPFC it is real and reactive power in given transmission line and voltage at the bus. Supplementary stabilising loop (lower part of figure) utilises state variables as input signals and, from the point of view of the whole system, is a state-variable control. State-variables can be measured by WAMS [10-13, 15].

The main problem for such a closed-loop control is the design of a state-variable control algorithm for a multi-machine power system model.

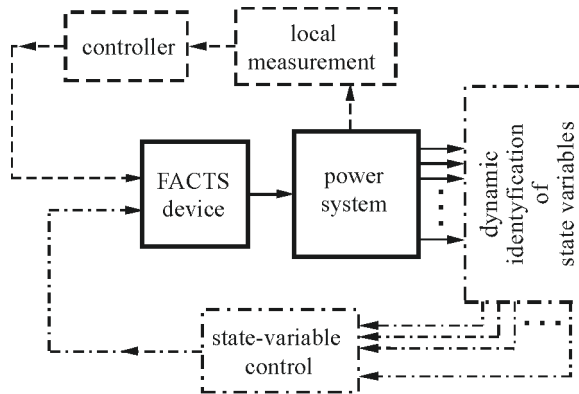


Fig. 1. Schematic illustration of the local and state-variable stabilising control

In order to derive the relevant control algorithm, the direct Lyapunov method has been applied to a multi-machine linear power system model. Direct Lyapunov method is a powerful tool for transient stability assessment and control of power system [2]. This paper extends the previous work of the authors [9, 18] on the design of Lyapunov-based damping controllers for shunt FACTS devices. Correctness of the derived state-variable control has been confirmed by computer simulation for a simple multi-machine test system. Further work is needed to address the problems related to fast measurement of input signals, real-time identification of system parameters, influence of more realistic models of generators and their AVRs, influence of different load models and their dynamics, and other implementation problems.

2. FACTS devices in tie-lines

UPFC, shown in Fig. 2a, consists of a shunt and series part. The shunt part consists of a supply (excitation) transformer ET and a voltage source converter CONV 1. The series part consists of a voltage source converter CONV 2 and a series (booster) transformer ST. Both voltage source converters CONV 1 and CONV 2 are connected back-to-back through the common dc link with a capacitor. Each converter has its own PWM controller which use two control parameters, respectively m_1, ψ_1 and m_2, ψ_2 . The shunt part of the UPFC works similarly as reactive power compensator STATCOM. Converter CONV 1 regulates voltage \underline{V}_{ac} and thereby also the current received by UPFC from the network. The voltage is expressed [1-3] by:

$$\underline{V}_{ac} = m_1 k V_{dc} (\cos \psi_1 + j \sin \psi_1). \quad (1)$$

The controller enforces a required value \underline{V}_{ac} by choosing appropriate values of m_1 and ψ_1 . The series part of the UPFC works similarly as series compensator. Converter CONV 2 regulates both the magnitude and the phase of the ac voltage $\Delta \underline{V}$ supplying the booster transformer. That voltage is expressed by:

$$\Delta \underline{V} = m_2 k V_{dc} (\cos \psi_2 + j \sin \psi_2). \quad (2)$$

The controller enforces the required value of $\Delta \underline{V}$ by choosing appropriate values of m_2 and ψ_2 . Thanks to controlling both the magnitude and the phase of the booster (series) voltage, the voltage \underline{V}_k at the beginning of the transmission line may assume any values within the circle created by the phasor \underline{V}_i , as illustrated on Fig. 2a. The simplified steady-state equivalent circuit (Fig. 2b) contains a series voltage source $\Delta \underline{V}$, reactance of the booster transformer X_{ST} , and shunt current source \underline{I}_{shunt} . Obviously the model must also include limiters for voltage ΔV and the allowed current flowing through the booster (series) transformer.

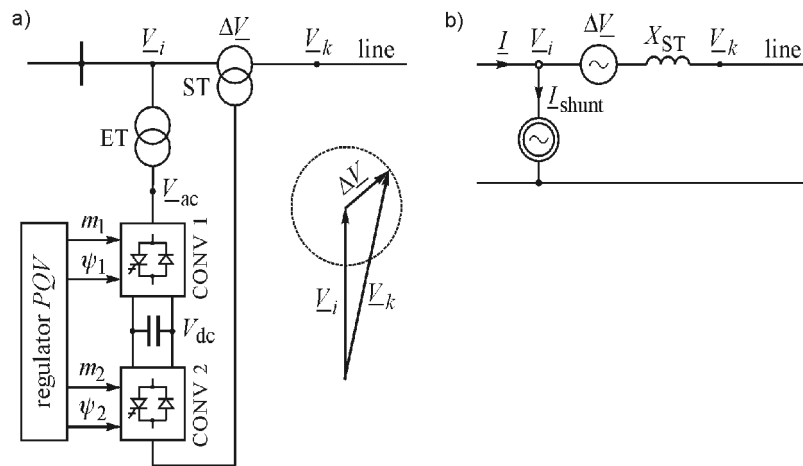


Fig. 2. Unified power flow controller (UPFC): (a) functional diagram and the phasor diagram; (b) equivalent circuit

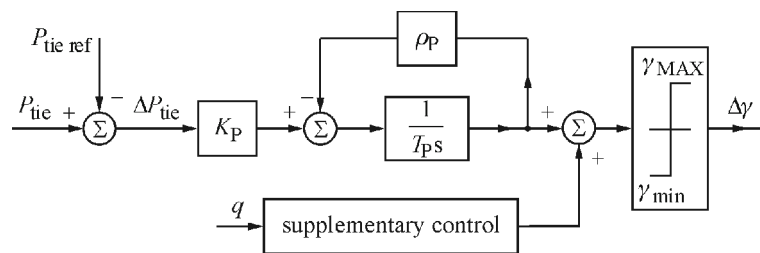


Fig. 3. Power flow controller installed in a tie-line of interconnected power system

Schematic diagram of a TCPAR regulator is shown in Fig. 3. An integral type regulator with negative feedback is placed in the main control path. The task of the regulator is regulating real power flow in the line in which the FACTS device is installed. The reference value is supplied from the supervisory control system. A supplementary control loop devoted to damping of power swings and improving power stability is shown in the lower part of the diagram.

3. Incremental model of transmission line

Figure 4 illustrates the stages of developing a model of the TCPAR installed in a tie-line. Booster voltage, which is in quadrature to the supply voltage, is injected in the transmission line using a booster transformer:

$$\Delta V_p = \gamma V_a, \quad (3)$$

where γ is the controlled variable. The booster transformer reactance has been added to the equivalent line reactance. To simplify considerations, the line and transformer resistances have been neglected.

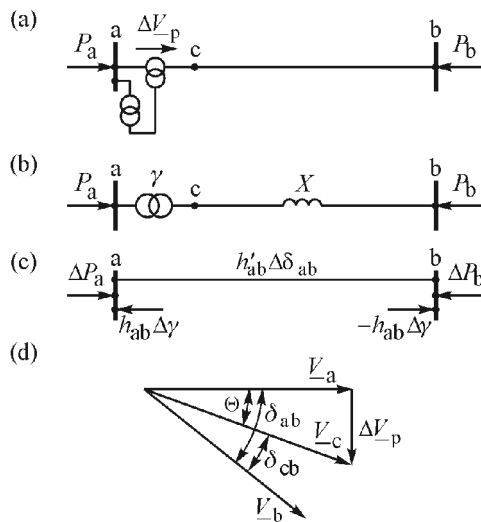


Fig. 4. Stages of developing an incremental model of a transmission line with a phase shifting transformer: (a) one-line diagram, (b) admittance model with ideal transformation ratio; (c) incremental model, (d) phasor diagram

The following relationships can be derived using the phasor diagram of Fig. 4d:

$$\sin \theta = \frac{\Delta V_p}{V_c} = \frac{\gamma V_a}{V_c}; \quad \cos \theta = \frac{V_a}{V_c}; \quad \delta_{cb} = \delta_{ab} - \theta. \quad (4)$$

Looking on the transmission line (Fig. 4d) from the side of node “a” it can be written that:

$$P_a = P_{ab} = P_{cb} = \frac{V_c V_b}{X} \sin \delta_{cb}. \quad (5)$$

Substituting (4) to the last equation gives:

$$\begin{aligned} P_a &= \frac{V_c V_b}{X} \sin(\delta_{ab} - \theta) = \frac{V_c V_b}{X} (\sin \delta_{ab} \cos \theta - \cos \delta_{ab} \sin \theta) = \\ &= \frac{V_a V_b}{X} \sin \delta_{ab} - \gamma \frac{V_a V_b}{X} \cos \delta_{ab}. \end{aligned} \quad (6)$$

That equation can also be written as:

$$P_a = P_{ab} = b_{ab} \sin \delta_{ab} - b_{ab} \cos \delta_{ab} \gamma(t), \quad (7)$$

where $b_{ab} = V_a V_b / X$ is the amplitude of the power-angle characteristic of the transmission line.

The values of variables at a given operating point are $(\hat{P}_a, \hat{\delta}, \hat{\gamma})$. Using those values, equation (7) gives:

$$\hat{P}_{ab} = \hat{P}_a = b_{ab} \sin \hat{\delta}_{ab} - b_{ab} \cos \hat{\delta}_{ab} \hat{\gamma}. \quad (8)$$

The tie-line flow in (7) depends on both the power angle δ_{ab} and the quadrature transformation ratio $\gamma(t)$. Hence in the vicinity of the operating point $(\hat{\delta}_{ab}, \hat{\gamma})$ it is obtained:

$$\Delta P_a = \frac{\partial P_a}{\partial \delta_{ab}} \Delta \delta_{ab} + \frac{\partial P_a}{\partial \gamma} \Delta \gamma, \quad (9)$$

where

$$\begin{aligned} \frac{\partial P_a}{\partial \delta_{ab}} &= b_{ab} \cos \hat{\delta}_{ab} + b_{ab} \sin \hat{\delta}_{ab} \hat{\gamma}, \\ \frac{\partial P_a}{\partial \gamma} &= -b_{ab} \cos \hat{\delta}_{ab}. \end{aligned} \quad (10)$$

Substituting partial derivatives (10) into (9) gives:

$$\Delta P_a = (b_{ab} \cos \hat{\delta}_{ab} + \hat{\gamma} b_{ab} \sin \hat{\delta}_{ab}) \Delta \delta_{ab} - (b_{ab} \cos \hat{\delta}_{ab}) \Delta \gamma. \quad (11)$$

The coefficients $b_{ab} \cos \hat{\delta}_{ab}$ and $b_{ab} \sin \hat{\delta}_{ab}$ in that equation are the same as those in (8). Component $b_{ab} \sin \hat{\delta}_{ab}$ can be eliminated from (11) using (8) in the following way. Equation (8) gives $b_{ab} \sin \hat{\delta}_{ab} = \hat{P}_{ab} + \hat{\gamma} b_{ab} \cos \hat{\delta}_{ab}$ or:

$$\hat{\gamma} b_{ab} \sin \hat{\delta}_{ab} = \hat{\gamma} \hat{P}_{ab} + \hat{\gamma}^2 b_{ab} \cos \hat{\delta}_{ab}. \quad (12)$$

Substituting that equation into (11) gives:

$$\Delta P_a = [(1 + \hat{\gamma}^2) (b_{ab} \cos \hat{\delta}_{ab}) + \hat{\gamma} \hat{P}_{ab}] \Delta \delta_{ab} - (b_{ab} \cos \hat{\delta}_{ab}) \Delta \gamma. \quad (13)$$

The following notation is introduced now:

$$h_{ab} = \frac{\partial P_a}{\partial \delta_{ab}} = b_{ab} \cos \hat{\delta}_{ab}, \quad (14)$$

$$h'_{ab} = (1 + \hat{\gamma}^2) (b_{ab} \cos \hat{\delta}_{ab}) + \hat{\gamma} \hat{P}_{ab} = (1 + \hat{\gamma}^2) h_{ab} + \hat{\gamma} \hat{P}_{ab}. \quad (15)$$

The variable h_{ab} given by (14) corresponds to the mutual synchronising power for the line "a-b" calculated neglecting the booster transformer and h'_{ab} given by (15) corresponds to the synchronising power when the booster transformer has been taken into account. Using that notation, equation (13) takes a form $\Delta P_a = h'_{ab} \Delta \delta_{ab} - h_{ab} \Delta \gamma$ or

$$\Delta P_a + h_{ab} \Delta \gamma = h'_{ab} \Delta \delta_{ab}. \quad (16)$$

Now, looking on the transmission line (Fig. 4d) from the side of node “b” it can be written that:

$$P_b = -P_{ab} = -P_{cb} = -\frac{V_c V_b}{X} \sin \delta_{cb}. \quad (17)$$

Linearization of this equation similar to (8) gives equation similar to (16), but with different signs:

$$\Delta P_b - h_{ab} \Delta \gamma = -h'_{ab} \Delta \delta_{ab}. \quad (18)$$

Substituting $\Delta \delta_{ab} = \Delta \delta_a - \Delta \delta_b$ into equations (16) and (18) it is easy to obtain two equivalent equations, which can be written in the following way:

$$\begin{bmatrix} \Delta P_a + h_{ab} \Delta \gamma \\ \Delta P_b - h_{ab} \Delta \gamma \end{bmatrix} = \begin{bmatrix} h'_{ab} & -h'_{ab} \\ -h_{ab} & h_{ab} \end{bmatrix} \begin{bmatrix} \Delta \delta_a \\ \Delta \delta_b \end{bmatrix}. \quad (19)$$

Equation (19) describes the incremental model of the transmission line shown in Fig. 4c. In that model there is an equivalent transmission line between nodes “a” and “b” with parameter h'_{ab} . Power injections in nodes “a” and “b” are $+h_{ab} \Delta \gamma$ and $-h_{ab} \Delta \gamma$, respectively. A change in the flow in that line corresponds to a change in the voltage angles $\Delta \delta_a$, $\Delta \delta_b$ at both nodes. Nodal power injections correspond to the flow changes due to the regulation of the quadrature transformation ratio $\gamma(t)$.

It will be shown later that the derived incremental model of a branch with a phase shifting transformer is convenient for the network analysis, especially for large networks, as it models changes in the quadrature transformation ratio by changes in power injections without changing parameters of the branches.

4. Incremental model of system

Analysing system frequency regulation, one can assume that changes in voltage magnitudes can be neglected and only changes in voltage angles are considered. Under this assumption it can be written that:

$$\Delta \mathbf{P} \cong \mathbf{H} \Delta \boldsymbol{\delta}, \quad (20)$$

where $\Delta \mathbf{P}$ and $\Delta \boldsymbol{\delta}$ are the vectors of changes in real power injections and voltage angles, respectively. Matrix \mathbf{H} is the Jacobi matrix and consist of partial derivatives $H_{ij} = \partial P_i / \partial \delta_j$. Equation (20) describes the incremental model of a network. Including a phase shifting transformer in the network incremental model is illustrated in Fig. 5. There are following node types:

{G} – generator nodes behind transient generator reactances,

{L} – load nodes,

a,b – terminal nodes of a line with a phase shifting transformer (as in Fig. 4).

The line with the phase shifting transformer (Fig. 5) is modelled using a transformation ratio and a branch. In the incremental model shown in Fig. 5 that line is modelled the way shown in Fig. 4. Matrix \mathbf{H} describing that network includes branch h'_{ab} from the incremental line model with the phase shifting transformer. There are real power injection in nodes “a” and “b”, similarly as in Fig. 4c, corresponding to flow changes due to transformation ratio regulation $\gamma(t)$.

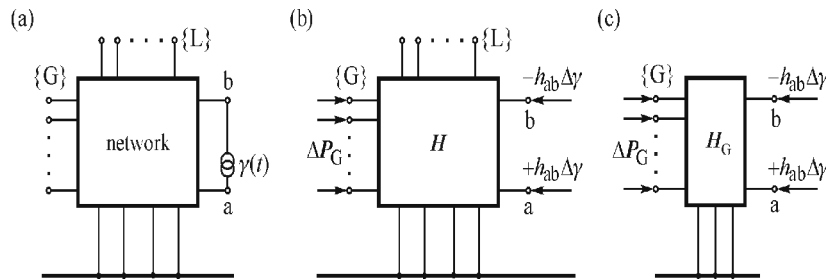


Fig. 5. Stages of developing the incremental model: (a) admittance model with a phase shifting transformer, (b) incremental model, (c) incremental model after elimination of nodes $\{L\}$

Now equation (20) describing the model shown in Fig. 5b can be expanded as:

$$\begin{bmatrix} \{G\} \\ a \\ b \\ \{L\} \end{bmatrix} \begin{bmatrix} \Delta P_G \\ +h_{ab}\Delta\gamma \\ -h_{ab}\Delta\gamma \\ \mathbf{0} \end{bmatrix} \cong \begin{bmatrix} \mathbf{H} \end{bmatrix} \begin{bmatrix} \Delta\delta_G \\ \Delta\delta_a \\ \Delta\delta_b \\ \Delta\delta_L \end{bmatrix}. \quad (21)$$

Substitution $\Delta P_L = \mathbf{0}$ has been made on the left-hand-side of (21) because loads at $\{L\}$ nodes are modelled as constant powers. Eliminating variables, related to load nodes $\{L\}$ in (21), by using the partial inversion method (described in [2]) makes it possible to transform equation (21) to the following form:

$$\begin{bmatrix} \{G\} \\ a \\ b \end{bmatrix} \begin{bmatrix} \Delta P_G \\ +h_{ab}\Delta\gamma \\ -h_{ab}\Delta\gamma \end{bmatrix} \cong \begin{bmatrix} \mathbf{H}_{GG} & \mathbf{H}_{Ga} & \mathbf{H}_{Gb} \\ \mathbf{H}_{aG} & \mathbf{H}_{aa} & \mathbf{H}_{ab} \\ \mathbf{H}_{bG} & \mathbf{H}_{ba} & \mathbf{H}_{bb} \end{bmatrix} \begin{bmatrix} \Delta\delta_G \\ \Delta\delta_a \\ \Delta\delta_b \end{bmatrix}. \quad (22)$$

That equation can be further transformed by partial inversion to the following equations:

$$\Delta P_G \cong \mathbf{H}_G \Delta\delta_G + [\mathbf{K}_{Ga} \quad \mathbf{K}_{Gb}] \begin{bmatrix} +h_{ab}\Delta\gamma \\ -h_{ab}\Delta\gamma \end{bmatrix}, \quad (23)$$

$$\begin{bmatrix} \Delta\delta_a \\ \Delta\delta_b \end{bmatrix} \cong - \begin{bmatrix} \mathbf{K}_{aG} \\ \mathbf{K}_{bG} \end{bmatrix} \Delta\delta_G + \begin{bmatrix} \mathbf{H}_{aa} & \mathbf{H}_{ab} \\ \mathbf{H}_{ba} & \mathbf{H}_{bb} \end{bmatrix}^{-1} \begin{bmatrix} +h_{ab}\Delta\gamma \\ -h_{ab}\Delta\gamma \end{bmatrix}, \quad (24)$$

where:

$$\mathbf{H}_G = \mathbf{H}_{GG} - [\mathbf{H}_{Ga} \quad \mathbf{H}_{Gb}] \begin{bmatrix} \mathbf{H}_{aa} & \mathbf{H}_{ab} \\ \mathbf{H}_{ba} & \mathbf{H}_{bb} \end{bmatrix}^{-1} \begin{bmatrix} \mathbf{H}_{aG} \\ \mathbf{H}_{bG} \end{bmatrix}, \quad (25)$$

$$[\mathbf{K}_{Ga} \quad \mathbf{K}_{Gb}] = [\mathbf{H}_{Ga} \quad \mathbf{H}_{Gb}] \begin{bmatrix} H_{aa} & H_{ab} \\ H_{ba} & H_{ba} \end{bmatrix}^{-1}, \quad (26)$$

$$\begin{bmatrix} \mathbf{K}_{aG} \\ \mathbf{K}_{bG} \end{bmatrix} = \begin{bmatrix} H_{aa} & H_{ab} \\ H_{ba} & H_{ba} \end{bmatrix}^{-1} \begin{bmatrix} \mathbf{H}_{aG} \\ \mathbf{H}_{bG} \end{bmatrix}. \quad (27)$$

Equations (23) and (24) describe the incremental model shown in Fig. 5c. Equation (23) describes how a change in the transformation ratio of a phase shifting transformer affects power changes in all generators. Equation (24) describes the influence of changes in the transformation ratio on the voltage angle changes in the terminal nodes of the line with the phase-shifting transformer. Equation (23) can be transformed to:

$$\Delta \mathbf{P}_G \cong \mathbf{H}_G \Delta \boldsymbol{\delta}_G + \Delta \mathbf{K}_{ab} h_{ab} \Delta \gamma, \quad (28)$$

where

$$\Delta \mathbf{K}_{ab} = \mathbf{K}_{Ga} - \mathbf{K}_{Gb}. \quad (29)$$

Hence a power change in the i -th generator can be expressed as:

$$\Delta P_i \cong \sum_{j \in \{G\}} H_{ij} \Delta \delta_j + \Delta K_i h_{ab} \Delta \gamma, \quad (30)$$

where $\Delta K_i = K_{ia} - K_{ib}$. Hence if $K_{ia} \cong K_{ib}$, then changes in $\Delta \gamma$ cannot influence power changes in i -th generator. In other words, that generator cannot be controlled using that phase shifting transformer. Coefficients K_{ia} , K_{ib} can be treated as measures of the distance from nodes “a” and “b” to the i -th generator. It means that if nodes “a” and “b” are at the same distance from the i -th generator then the device cannot influence that generator. That can be checked using Fig. 5c, as power injections in nodes “a” and “b” have opposite signs. Hence if the distances are the same, then the influences on that generator compensate each other out. Swings of the generator rotors are described by the following equations [2]:

$$\frac{d\Delta \delta_i}{dt} = \Delta \omega_i, \quad (31)$$

$$M_i \frac{d\Delta \omega_i}{dt} = -\Delta P_i - D_i \Delta \omega_i$$

for $i \in \{G\}$. As the network equations were derived in the matrix form, it is convenient to write the above equation in the matrix form too:

$$\Delta \dot{\boldsymbol{\delta}}_G = \Delta \boldsymbol{\omega}_G, \quad (32)$$

$$\mathbf{M} \Delta \dot{\boldsymbol{\omega}}_G = -\Delta \mathbf{P}_G - \mathbf{D} \Delta \boldsymbol{\omega}_G,$$

where \mathbf{M} , \mathbf{D} are diagonal matrices of respectively the inertia and damping coefficients, and $\Delta \boldsymbol{\delta}_G$, $\Delta \boldsymbol{\omega}_G$, $\Delta \mathbf{P}_G$ are column matrices of respectively changes in rotor angles, rotor speed deviations, and real power generations.

Substituting (28) to the second equation of (32) gives the following state equation:

$$\mathbf{M}\Delta\dot{\boldsymbol{\omega}}_G = -\mathbf{H}_G\Delta\boldsymbol{\delta}_G - \mathbf{D}\Delta\boldsymbol{\omega}_G - \Delta\mathbf{K}_{ab} h_{ab} \Delta\gamma(t). \quad (33)$$

Here $\Delta\gamma(t)$ is the control function corresponding to the transformation ratio change of the phase shifting transformer. Function $\Delta\gamma(t)$ affects motions of each rotor proportionally to coefficient $\Delta K_i h_{ab} = (K_{ia} - K_{ib})h_{ab}$.

The main question now is how $\Delta\gamma(t)$ should be changed so that a control of a phase-shifting transformer improves damping of oscillations. The control algorithm of $\Delta\gamma(t)$ will be derived using the Lyapunov direct method.

5. State-variable control in general case

In [2, 16,17] the total system energy $V(\boldsymbol{\delta}, \boldsymbol{\omega}) = \mathbf{E}_k + \mathbf{E}_p$ was used as the Lyapunov function in the non-linear system model (with line conductances neglected). In the considered linear model (33) the total system energy can be expressed as the sum of rotor speed and angle increments. That corresponds to expanding $V(\boldsymbol{\delta}, \boldsymbol{\omega}) = \mathbf{E}_k + \mathbf{E}_p$ in Taylor series in the vicinity of an operating point. That equation shows that $V(\mathbf{x})$ can be approximated in a vicinity of an operating point using a quadratic form based on the Hessian matrix of function $V(\mathbf{x})$.

For the potential energy \mathbf{E}_p the Hessian corresponds to the gradient of real power generations and therefore also the Jacobian matrix used in the above incremental model.

$$\left[\frac{\partial^2 \mathbf{E}_p}{\partial \delta_i \partial \delta_j} \right] = \left[\frac{\partial P_i}{\partial \delta_j} \right] = \mathbf{H}_G. \quad (34)$$

Hence, it can be proved that:

$$\Delta \mathbf{E}_p = \frac{1}{2} \Delta \boldsymbol{\delta}_G^T \mathbf{H}_G \Delta \boldsymbol{\delta}_G. \quad (35)$$

It was shown in [2] that if the network conductances were neglected, matrix \mathbf{H}_G is positive-definite at an operating point (stable equilibrium point). Hence the quadratic form (35) is also positive definite.

The kinetic energy \mathbf{E}_k can be expressed as:

$$\Delta \mathbf{E}_k = \frac{1}{2} \Delta \boldsymbol{\omega}_G^T \mathbf{M} \Delta \boldsymbol{\omega}_G. \quad (36)$$

It is a quadratic form made up of the vector of speed changes and a diagonal matrix of inertia coefficients. Matrix \mathbf{M} is positive definite, so the above quadratic form is also positive definite.

Total energy increment $\Delta V(\boldsymbol{\delta}, \boldsymbol{\omega}) = \Delta \mathbf{E}_k + \Delta \mathbf{E}_p$ is given by:

$$\Delta V = \Delta \mathbf{E}_k + \Delta \mathbf{E}_p = \frac{1}{2} \Delta \boldsymbol{\omega}_G^T \mathbf{M} \Delta \boldsymbol{\omega}_G + \frac{1}{2} \Delta \boldsymbol{\delta}_G^T \mathbf{H}_G \Delta \boldsymbol{\delta}_G. \quad (37)$$

That function is positive definite as the sum of positive-definite functions and therefore it can be used as a Lyapunov function providing its time derivative at the operating point is negative definite. Differentiating (35) and (36) gives:

$$\Delta \dot{E}_p = \frac{1}{2} \Delta \omega_G^T \mathbf{H}_G \Delta \delta_G + \frac{1}{2} \Delta \delta_G^T \mathbf{H}_G \Delta \omega_G, \quad (38)$$

$$\Delta \dot{E}_k = \frac{1}{2} \Delta \dot{\omega}_G^T \mathbf{M} \Delta \omega_G + \frac{1}{2} \Delta \omega_G^T \mathbf{M} \Delta \dot{\omega}_G. \quad (39)$$

Now, it is useful to transpose equation (33):

$$\Delta \dot{\omega}_G^T \mathbf{M} = -\Delta \delta_G^T \mathbf{H}_G - \Delta \omega_G^T \mathbf{D} - \Delta \mathbf{K}_{ab}^T h_{ab} \Delta \gamma(t). \quad (40)$$

Substituting right-hand-side of (40) for $\Delta \dot{\omega}_G^T \mathbf{M}$ in the first component of (39) gives:

$$\begin{aligned} \Delta \dot{E}_k = & -\frac{1}{2} \Delta \delta_G^T \mathbf{H}_G \Delta \omega_G - \frac{1}{2} \Delta \omega_G^T \mathbf{H}_G \Delta \delta_G - \Delta \omega_G^T \mathbf{D} \Delta \omega_G + \\ & -\frac{1}{2} (\Delta \mathbf{K}_{ab}^T \Delta \omega_G + \Delta \omega_G^T \Delta \mathbf{K}_{ab}) h_{ab} \Delta \gamma(t). \end{aligned} \quad (41)$$

It can be easily checked that both expressions in the last component of (41) are identical scalars as:

$$\Delta \mathbf{K}_{ab}^T \Delta \omega_G = \Delta \omega_G^T \Delta \mathbf{K}_{ab} = \sum_{i \in \{G\}} \Delta K_i \Delta \omega_i. \quad (42)$$

Hence equation (41) can be re-written as:

$$\Delta \dot{E}_k = -\frac{1}{2} \Delta \delta_G^T \mathbf{H}_G \Delta \omega_G - \frac{1}{2} \Delta \omega_G^T \mathbf{H}_G \Delta \delta_G - \Delta \omega_G^T \mathbf{D} \Delta \omega_G - \Delta \mathbf{K}_{ab}^T \Delta \omega_G h_{ab} \Delta \gamma(t). \quad (43)$$

Adding both sides of (43) and (38) gives:

$$\Delta \dot{V} = \Delta \dot{E}_k + \Delta \dot{E}_p = -\Delta \omega_G^T \mathbf{D} \Delta \omega_G - \Delta \mathbf{K}_{ab}^T \Delta \omega_G h_{ab} \Delta \gamma(t). \quad (44)$$

In a particular case when there is no control, i.e. when $\Delta \gamma(t) = 0$, equation in (44) gives:

$$\Delta \dot{V} = \Delta \dot{E}_k + \Delta \dot{E}_p = -\Delta \omega_G^T \mathbf{D} \Delta \omega_G. \quad (45)$$

As matrix \mathbf{D} is positive definite, the function above is negative definite. Hence function (37) can be treated as the Lyapunov function. In order that the considered system is stable when $\Delta \gamma(t) \neq 0$ is changing, the second component in (44) should be always positive:

$$\Delta \mathbf{K}_{ab}^T \Delta \omega_G h_{ab} \Delta \gamma(t) \geq 0. \quad (46)$$

That can be ensured using the following control algorithm:

$$\Delta\gamma(t) = \kappa h_{ab} \Delta \mathbf{K}_{ab}^T \Delta \boldsymbol{\omega}_G. \quad (47)$$

With that control algorithm the derivative (44) of the Lyapunov function is given by:

$$\Delta \dot{V} = -\Delta \boldsymbol{\omega}_G^T \mathbf{D} \Delta \boldsymbol{\omega}_G - \kappa (h_{ab} \Delta \mathbf{K}_{ab}^T \Delta \boldsymbol{\omega}_G)^2 \leq 0, \quad (48)$$

where κ is the control gain. Taking into account (42), the control algorithm (47) can be written as:

$$\Delta\gamma(t) = \kappa h_{ab} \sum_{i \in \{G\}} \Delta K_i \Delta \omega_i, \quad (49)$$

where $\Delta K_i = K_{ia} - K_{ib}$. That control algorithm is valid for any location of the phase shifting transformer.

In the particular case when the phase shifting transformer is located in a tie-line the control law can be simplified as described below.

6. State-variable control for TCPAR in tie-line

It is assumed now that considered interconnected power system consists of three subsystems (control areas) as illustrated in Fig. 6. The set $\{G\}$ of the generator nodes is divided into three subsets corresponding that subsystems: $\{G\} = \{G_A\} + \{G_B\} + \{G_C\}$.

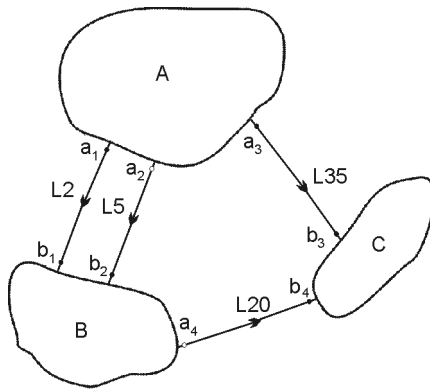


Fig. 6. A three area test system with tie-lines L2, L5, L20, L35

Now the summation in equation (49) can be divided into three sums:

$$\Delta\gamma(t) = \kappa h_{ab} \sum_{i \in \{G_A\}} \Delta K_i \Delta \omega_i + \kappa h_{ab} \sum_{i \in \{G_B\}} \Delta K_i \Delta \omega_i + \kappa h_{ab} \sum_{i \in \{G_C\}} \Delta K_i \Delta \omega_i. \quad (50)$$

Following a disturbance in one of the subsystems, there are local swings of generator rotors inside each subsystem and inter-area swings of subsystems with respect to each other. The frequency of local swings is about 1 Hz while the frequency of inter-area swings is much

lower, usually about 0.25 Hz. Hence when investigating the inter-area swings, the local swings can be approximately neglected. Therefore it can be assumed that:

$$\begin{aligned} \Delta\omega_1 \cong \dots = \Delta\omega_i \cong \dots \cong \Delta\omega_{n_A} &\cong 2\pi \Delta f_A \quad \text{for } i \in \{G_A\}, \\ \Delta\omega_1 \cong \dots = \Delta\omega_i \cong \dots \cong \Delta\omega_{n_B} &\cong 2\pi \Delta f_B \quad \text{for } i \in \{G_B\}, \\ \Delta\omega_1 \cong \dots = \Delta\omega_i \cong \dots \cong \Delta\omega_{n_C} &\cong 2\pi \Delta f_C \quad \text{for } i \in \{G_C\}. \end{aligned} \quad (51)$$

Now equation (48) can be expressed as:

$$\Delta\gamma(t) = \kappa 2\pi h_{ab} \left[\Delta f_A \sum_{i \in \{G_A\}} \Delta K_i + \Delta f_B \sum_{i \in \{G_B\}} \Delta K_i + \Delta f_C \sum_{i \in \{G_C\}} \Delta K_i \right], \quad (52)$$

or, after summing the coefficients:

$$\Delta\gamma(t) = \kappa 2\pi h_{ab} (\Delta K_A \Delta f_A + \Delta K_B \Delta f_B + \Delta K_C \Delta f_C), \quad (53)$$

where:

$$\Delta K_A = \sum_{i \in \{G_A\}} \Delta K_i, \quad \Delta K_B = \sum_{i \in \{G_B\}} \Delta K_i, \quad \Delta K_C = \sum_{i \in \{G_C\}} \Delta K_i. \quad (54)$$

Equation (53) shows that the control of a phase shifting transformers should employ the signals of frequency deviations weighted by coefficients (54). Block diagram of the supplementary control loop based on (53) is shown in Fig. 7. The way the supplementary control loop is added to the overall regulator has been shown earlier in Fig. 3.

The sign of gains ΔK_A , ΔK_B , ΔK_C in equation (52) and Fig. 7 are positive or negative. Moreover an important property can be proved, that the sum of these gains is equal to zero: $(\Delta K_A + \Delta K_B + \Delta K_C) = 0$. As a result of this property, in the case when all control areas change the frequency simultaneously $\Delta f_A = \Delta f_B = \Delta f_C$, the control output signal is equal to zero: $\Delta\gamma(t) = 0$. It is correct, because the stabilising control should act only in the case when there are power swigs between control areas and $\Delta f_A \neq \Delta f_B \neq \Delta f_C$.

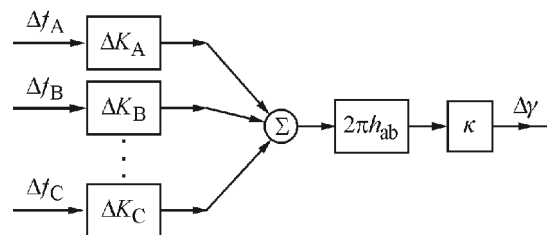


Fig. 7. Block diagram of the stabilising control loop of a power flow controller installed in a tie-line of an interconnected power system

The input signals to the supplementary control are frequency deviations Δf in each subsystem. Those signals should be transmitted to the regulator using telecommunication links

or a wide-area measurement system (WAMS) [10-15]. For the frequency of inter-area swings of about 0.25 Hz the period of oscillations is about 4 seconds and the speed of signal transmission to the regulator does not have to be high. It is enough if the signals are transmitted every 0.1 seconds, which is not a tall order for modern telecom systems.

The coefficients h_{ab} , ΔK_A , ΔK_B , ΔK_C in (53) have to be calculated by an appropriate SCADA/EMS function using current state estimation results and system configuration. Obviously those calculation do not have to be repeated frequently. Modifications have to be done only after system configuration changes or after a significant change of power system loading.

When deriving equation (53), for simplicity only one phase-shifting transformer was assumed. Similar considerations can be undertaken [18] for any number of phase-shifting transformers installed in any number of tie-lines. For each transformer, identical control laws are obtained but obviously with different coefficients calculated for respective tie-lines.

7. Test results for New England Test System

Simulation tests of the proposed supplementary control of TCPAR's installed in tie-lines have been done for a Modified New England Test System (10 generators 31 nodes, 38 branches). It has been divided into three subsystems, each of them being a control area with its own LFC. Control areas are connected as shown in Fig. 6 and Fig. 8. Detailed data and models of power system elements are described in [18].

Compared to the original New England Test System, the modified version has extended tie-line in order to reduce the frequency of tie-line oscillations to a more realistic value. In the modified system the frequency of inter-area swings is about 0.5 Hz while the frequency of swings of machine within the areas is about 1 Hz.

It is assumed that there are two TCPARs installed in the places marked in Fig. 6a by little blank circles – one in line L5 near node a_2 (node B3 in Fig. 8) and one in line L20 near node a_4 (node B15 in Fig. 8). Considered disturbance appears in area B and consists of an outage of a 250 MW generating unit (tripped by a generator protection).

Figure 9 shows the variation of the frequency in area B. A thick line shows the response when two (above mentioned) TCPARs were active and a thin line the response when TCPARs were not active. When TCPARs are not active, the frequency is affected by inter-area oscillations (the thin line). Active TCPARs (controlled with the use of the proposed method) quickly damp out the inter-area oscillations and the frequency variation is much smoother (the thick line). Frequency response for area A and area C is similar.

Dynamic response of real power in the tie-lines for the same disturbance, as discussed above, is shown in Fig. 10. When the TCPARs are not active in all tie-line the inter-area power swings are observable (the thin line). Active TCPARs (controlled using the proposed method) quickly damp out the inter-area oscillations and the dynamic response is almost aperiodic (the thick line).

In considered example the active TCPARs have a slight effect on the response of the mechanical (turbine) power. For several seconds the control areas A and C support area B by

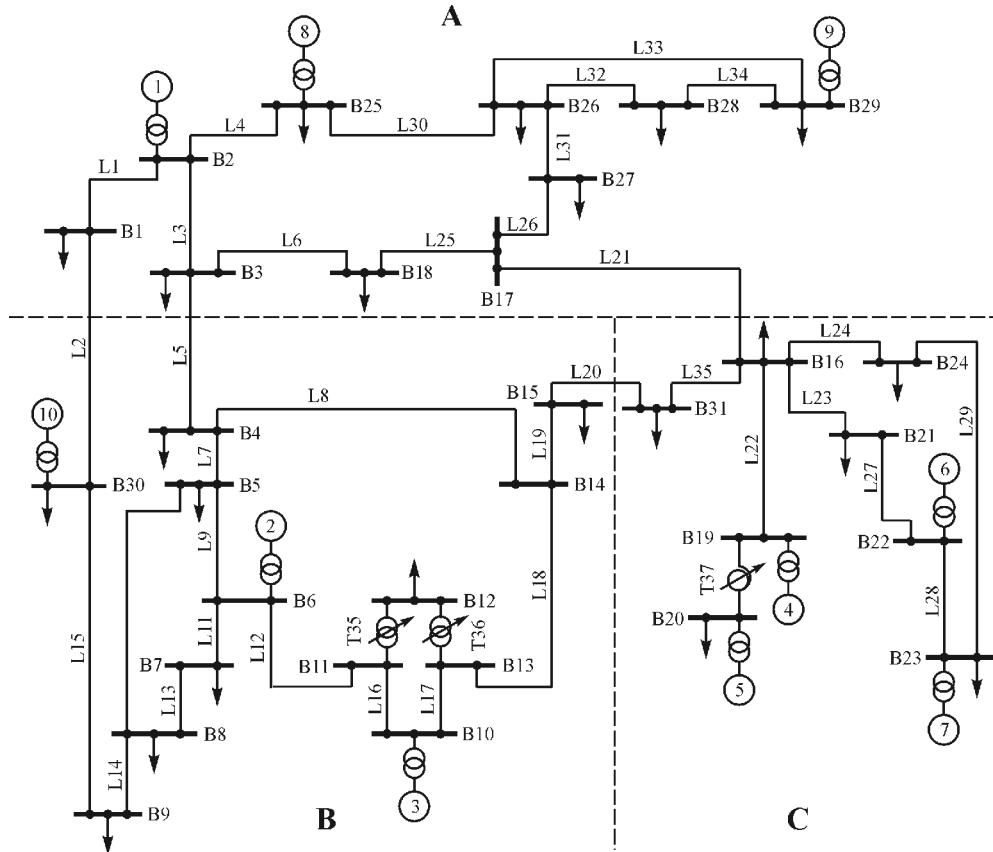


Fig. 8. Modified New England Test System

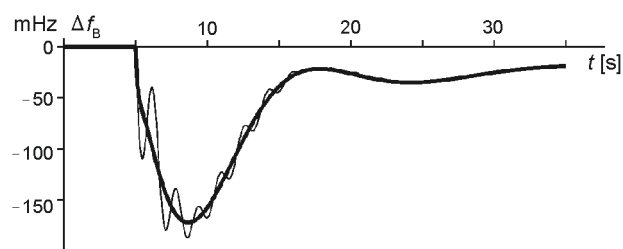


Fig. 9. Time response of frequency in Area B for considered disturbance

means of power injection. As frequency returns to its reference value, the area B increases its generation and the areas A and C withdraw their support.

Dissertation [18] contains many simulation results for all possible placements of TCPARs in the tie-lines. The results are similar as those presented here and confirm the efficiency of the proposed supplementary control.

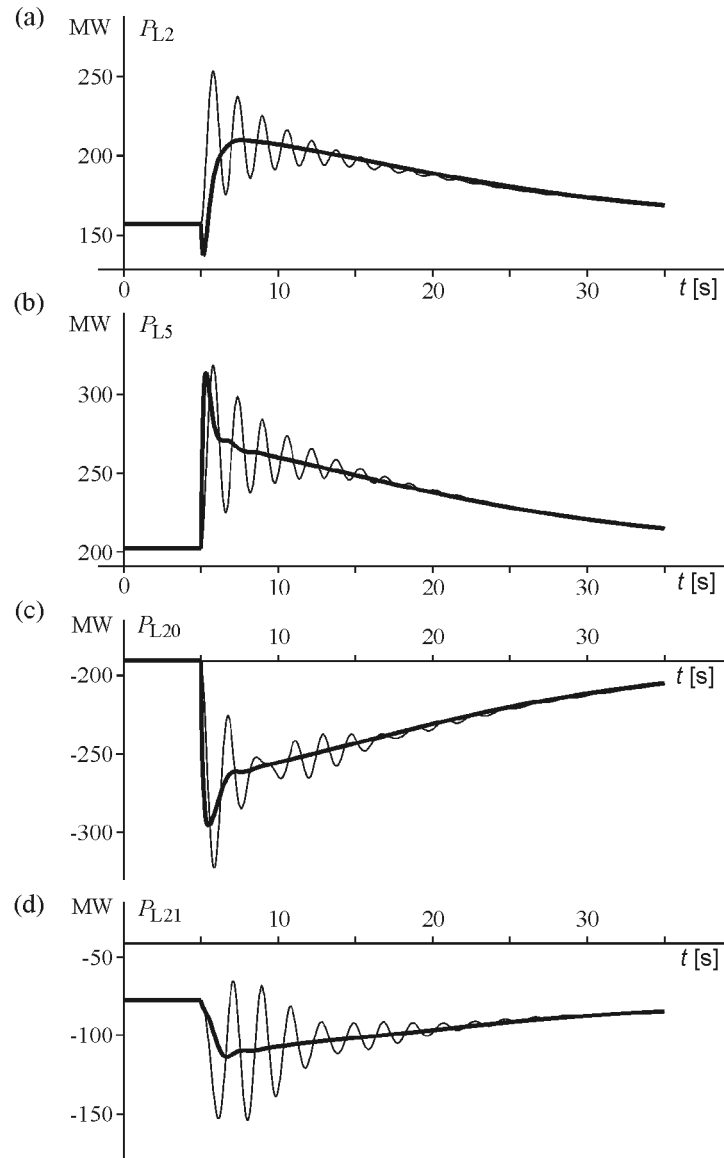


Fig. 10. Time response of real power in the tie-lines for considered disturbance

6. Modal analysis

This section presents the results of modal analysis for the considered test network – refer to [18] for full details. Figure 11 shows eigenvalue loci for the localization of TCPARs considered in Fig. 9 and Fig. 10, i.e. for TCPARs installed in tie-lines L5 and L20.

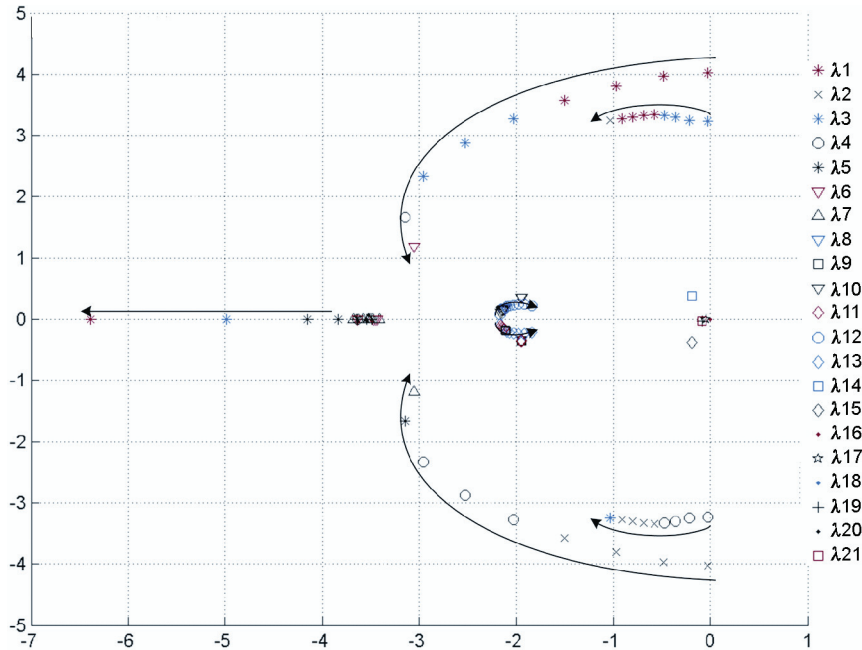


Fig. 11. Eigenvalue loci for test system with TCPAR's installed in the tie-lines L5 and L20

The calculations started from a very small value of the control gain κ in equation (47). Figure 11 shows that when the value of the gain κ was increased, the eigenvalues moved to the left hence enhancing stability of the system.

Analysis using participation factors, see [2], demonstrates that the eigenvalues shown in Fig. 11 are mainly connected with frequency deviations $\Delta f_A, \Delta f_B, \Delta f_C$ in all control areas and with power angles $\Delta \delta_A, \Delta \delta_B, \Delta \delta_C$ of the equivalent generators representing these areas (Fig. 6).

The results of modal analysis shown here and reported in [18] confirm strong influence of the proposed supplementary stabilising control on damping of the inter-area oscillations.

7. Robustness of the proposed control

The coefficients $h_{ab}, \Delta K_A, \Delta K_B, \Delta K_C$ in the multi-input stabilising control loop (Fig. 7) depend on the power system parameters and have to be calculated by an appropriate SCADA/EMS function using current state estimation results and system configuration.

Obviously in practice calculation of $h_{ab}, \Delta K_A, \Delta K_B, \Delta K_C$ may not be frequent in order not to overload SCADA/EMS. Moreover it is doubtful whether the values of $h_{ab}, \Delta K_A, \Delta K_B, \Delta K_C$ can be updated quickly enough, to follow the system transient trajectory, following a disturbance. Hence a question arises whether the proposed methodology is robust to

the changes of system parameters if the values of h_{ab} , ΔK_A , ΔK_B , ΔK_C cannot be updated quickly enough.

Dissertation [18] shows simulation results for many disturbances when the values of coefficients h_{ab} , ΔK_A , ΔK_B , ΔK_C are kept constant as in the pre-fault conditions. The results confirm the robustness of the proposed methodology.

To demonstrate that, Fig. 12 shows simulation results when TCPARs were installed in lines L5 and L20, i.e. the same situation as that shows in Fig. 10. It was assumed that a disturbance appears in area B and consists of an outage of a 250 MW generating unit (tripped by a generator protection). To test robustness of the methodology to the changes in values of h_{ab} , ΔK_A , ΔK_B , ΔK_C , it was additionally assumed that line L6 in system A (close to lone L5 and node node B15 in Fig. 8) is outaged. The solid line in Fig. 12 shows time response of real power in tie-line L5 when the values of h_{ab} , ΔK_A , ΔK_B , ΔK_C have been updated after Line L6 was outaged while the dotted line shows the case when the values of the coefficients were kept constant. A comparison between the two responses shows that the error in calculation of the coefficients did not influence the dynamic system response in a significant manner.

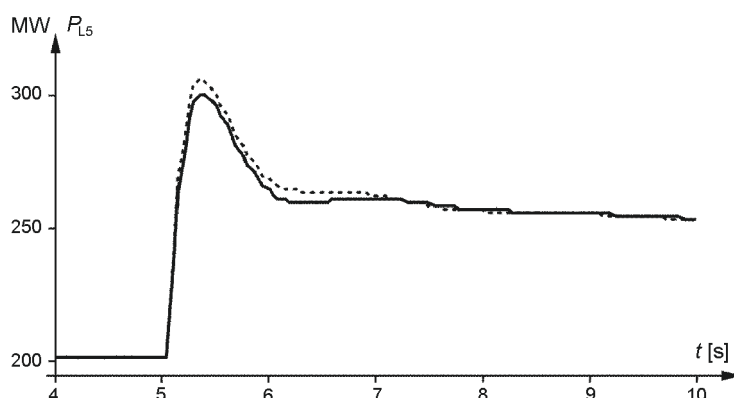


Fig. 12. Comparison of the time response in the case when control parameters are updated (solid line) and kept constant (dotted line)

It should be emphasised that the robustness of the control strategy to the changes in system parameters is due to the fact that the control is based on signals coming from all parts of the system. This is not possible when the control is based on local measurements.

8. Conclusions

This paper addressed the problem of a state-variable stabilising control of power system using series FACTS devices such as TCPAR or UPFC operating with quadrature booster regulation. It is assumed that these type of FACTS devices are installed in the tie-lines of an interconnected power system.

A control strategy for a multi-machine linear system model in such a case has been derived using energy-type Lyapunov function with the aim of maximising the rate of energy dissipation during power swings. Validity of the proposed stabilising control has been confirmed by computer simulation for a multi-machine test system and modal analysis.

It was shown that the proposed supplementary stabilising control is robust to the changes in system parameters. This is due to using a multi-input control based on signals coming from each control area.

Further research is needed to check the influence of different load models, load dynamics, more realistic models of generators and their AVR and PSSs, interactions with other controllers, inaccuracies in signals, time delays etc.

Acknowledgement

The research was supported by a research project No N N511 349637 financed by Ministry of Science and Higher Education of Poland.

References

- [1] Hingorani N.G., Gyugyi L. *Understanding FACTS. Concepts and Technology of Flexible AC Transmission Systems*. IEEE Press (2000).
- [2] Machowski J., Bialek J., Bumby J. *Power System Dynamics. Stability and Control*, John Wiley & Sons, Chichester (2008).
- [3] CIGRE Technical Brochure, No 145: *Modelling of power electronics equipment (FACTS) in load flow and stability programs*. <http://www.e-cigre.org>
- [4] Youke Lin Tan, Wang Youyi: *Design of series and shunt FACTS controller using adaptive non-linear coordinated design techniques*. IEEE Transaction on Power Systems 12(3) (1997).
- [5] Wang F.F., Swift F.J., Li M. *A unified model for the analysis of FACTS devices in damping power system oscillations. II. Multi-machine power systems*. IEEE Trans. Power Delivery 13: 1355-1362 (1998).
- [6] Pal B.C., Coonick A.H., Jaimoukha I.M., El-Zobaidi H. *A linear matrix inequality approach to robust damping control design in power systems with superconducting magnetic energy storage device*. IEEE Transactions on Power Systems 15 (2000).
- [7] Chaudhuri B., Pal B.C., Zolotas A.C. et al. *Mixed-sensitivity approach to H_{∞} control of power system oscillations employing multiple FACTS devices*. IEEE Trans. Power Systems 18: 1149-1156 (2003).
- [8] Kamwa I., Gerin-Lajoie L., Trudel G. *Multi-Loop Power System Stabilizers Using Wide-Area Synchronous Phasor Measurements*. Proceedings of the American Control Conference, Philadelphia Pennsylvania (1998).
- [9] Machowski J., Bialek J. *State-variable control of shunt FACTS devices using phasor measurements*. Electric Power System Research 78, Issue 1: 39-48 (2008).
- [10] Bhargava B. *Synchronised phasor measurement system project at Southern California Edison Co*. IEEE PES Summer Meeting 1: 16-22 (1999).
- [11] Magnus A., Karlsson D. *Phasor measurement applications in Scandinavia*. Transmission and Distribution Conference and Exhibition 2002: Asia Pacific. IEEE/PES 1: 480-484 (2002).
- [12] Yu C.S., Liu C.W. *Self-correction two-machine equivalent model for stability control of FACTS system using real-time phasor measurements*. IEE Proc. Gen., Transm. and Distrib. 149: 389-396 (2002).
- [13] Kamwa I., Grondin R., Hebert Y. *Wide-area measurement based stabilising control of large power systems – a decentralized/hierarchical approach*. IEEE Trans. Power Systems 16: 136-153 (2001).

-
- [14] Aboul-Ela M.E., Sallam A.A., McCalley J. D., Fouad A.A. *Damping controller design for power system oscillations using global signals*. IEEE Trans., Power Systems 11: 767-773 (1996).
 - [15] Adamiak M.G., Apostolov A.P., Begovic M.M. et al. *Wide Area Protection-Technology and Infrastructures*. IEEE Trans. Power Delivery 21: 601-609 (2006).
 - [16] Pai M.A. *Energy Function Analysis For Power System Stability*. Kluwer Academic Publishers (1989).
 - [17] Pavella M., Ernst D., Ruiz-Vega D. *Transient Stability of Power Systems. A unified Approach to Assessment and Control*, Kluwer's Power Electronics and Power System Series, SECS581 0-7923-7963-2 (2000).
 - [18] Nogal L. *Control of series FACTS devices by the use of WAMS*. Ph D Thesis, Warsaw University of Technology (2009) (in Polish).
 - [19] Zarghami M., Crow M.L., Sarangapani J. et al. *A Novel Approach to Inter-area Oscillation Damping by Unified Power Flow Controllers Utilizing Ultracapacitors*. IEEE Trans. Power Systems 25(1): 404-412 (2010).